

# Optimal imitation capacity and crossover phenomenon in the dynamics of social contagions

Xuzhen Zhu<sup>1</sup>, Wei Wang<sup>2</sup>, Shimin Cai<sup>3,4</sup>  
and H Eugene Stanley<sup>5</sup>

<sup>1</sup> State Key Laboratory of Networking and Switching Technology, Beijing University of Posts and Telecommunications, Beijing 100876, People's Republic of China

<sup>2</sup> Cybersecurity Research Institute, Sichuan University, Chengdu 610065, People's Republic of China

<sup>3</sup> School of Computer Science and Engineering, University of Electronic Science and Technology of China, Chengdu 611731, People's Republic of China

<sup>4</sup> Big Data Research Center, University of Electronic Science and Technology of China, Chengdu 611731, People's Republic of China

<sup>5</sup> Center for Polymer Studies and Department of Physics, Boston University, Boston, MA 02215, United States of America

E-mail: [wwzqbx@hotmail.com](mailto:wwzqbx@hotmail.com)

Received 24 March 2018

Accepted for publication 25 May 2018

Published 20 June 2018



Online at [stacks.iop.org/JSTAT/2018/063405](https://stacks.iop.org/JSTAT/2018/063405)  
<https://doi.org/10.1088/1742-5468/aac914>

**Abstract.** In the threshold model of social contagions with non-redundant memory, researchers have overlooked the investigation on the limited imitation (LI) effect, which shows individual imitates the behavior adoption only for a certain range of ratio of his adopted informants. To understand such LI effect, we propose a social contagion model with a gate-like adoption probability consisting of the 'on' and 'off' thresholds. With extensive numerical simulations, we find that, given information transmission probability and a gate width (the 'off' threshold minus the 'on' threshold), there exists an optimal imitation capacity with the optimal 'on' threshold maximizing the final adoption size. And the large 'off' threshold serves for further enlarging the final adoption size at a given 'on' threshold. Besides, a cross phenomenon in phase transition is also uncovered: the increase of 'on' threshold causes the growth pattern of

final behavior adoption size versus the information transmission probability change from the second-order to the first-order phase transition. We finally find that the above phenomena are qualitatively unaffected by the heterogeneity level of degree distribution. At last, an edge-based compartmental theory is conceived for theoretical analysis. And our suggested theory agrees well with the simulation results.

**Keywords:** network dynamics, nonlinear dynamics

---

**Contents**

<b>1. Introduction</b>	<b>2</b>
<b>2. Social contagion model with LI effect</b>	<b>4</b>
<b>3. Numerical results</b>	<b>5</b>
<b>4. Theoretical analysis based on edge-based compartmental theory</b>	<b>11</b>
<b>5. Conclusions</b>	<b>16</b>
<b>Acknowledgments</b> .....	<b>17</b>
<b>References</b>	<b>17</b>

---

**1. Introduction**

Nowadays, owing to the remarkable significance of social network, more and more researchers have greatly contributed to social contagion in terms of network science [1, 2]. Unlike epidemic spreading [3–8], social contagion exhibits distinctive reinforcement characteristic [9]. An effective method to depict the reinforcement in social contagion is threshold model [10, 12–15] that assumes an individual will adopt the information or behavior when the number or fraction of his adopted neighbors exceeds the adoption threshold. During the exploration of social contagion, considerable efforts are devoted to the studies of behavior spreading [16, 17], information spreading [18, 19], influence spreading [20] and the contagion of sentiment [21] to theoretically and experimentally unveil the essential nature of social contagions [21, 22]. In particular, behavior spreading attracts more interest and is widely modeled as a trivial Markovian process. Extensive numerical simulations and theoretical analyses have discovered that the social reinforcement effect can transform the phase transitions of social contagions [10, 11]. Especially, the final adoption size first grows continually and then decreases discontinuously versus the average degree. Recently, many non-Markovian models have also been proposed to describe another novel social reinforcement effect [23–33]. Wang *et al* have proposed a novel model with social reinforcement originating in the memory of non-redundant information transmission [25], which means information is disallowed to be retransmitted to a neighbor along the same edge after a successful transmission. In such condition, the growth of the final adoption size depends on the behavior

information transmission probability, and it changes from a continuous to a discontinuous pattern when the dynamical or structural parameters are altered.

In reality, whether an individual will adopt a behavior positively or negatively depends on the number of neighbors who have already adopted the behavior. For example, a shrewd businessman will imitate precursory achievers to invest scarce business to earn a great deal of profit when there are few business participants, and abandon the gainless business when a large quantity of followers conduct the same business (Leibenstein calls this the ‘snob effect’ [34]). Another example is when an individual habitually patronizes a park with good exercise and a convivial atmosphere, but then avoids it when it becomes overly-popular and jam-packed. Both of these examples embody the limited imitation (LI) effect [35–37], i.e. an individual adopts the behavior with the probability 1 at a critical number or fraction of adopted informants, and abandons the behavior after a certain increase of number or fraction. Different from LI effect, the EI Farol problem in minority games assumes that an agent will take the behavior even if there is globally no adopter and abandon the behavior only if the adopted fraction exceeds a critical point, markedly affecting the emergence of global cooperation [38–41]. Both the LI effect and EI Farol problem have a non-homogenous growth of the adoption probability with the number of adoptees in the neighborhood (or in the whole population). Doddes in [37] finds significant variation in the limiting behavior of a population’s infected fraction, ranging from steady state to chaotic.

In respect of non-redundant memory, however, LI effect disappointedly lacks systematical investigation. To this point, we provide a social contagion model leveraging non-Markovian property to describe the dynamics of behavior spreading with LI effect. We (based on LI effect) build a stochastic model for social contagion dynamics, considering social reinforcement in terms of non-redundant memory. In our model, information indicates the behavioral information. The non-redundant memory consists of two attributes: (1) non-redundant information transmission, i.e. disallowing information retransmission alongside the same edge after a successful transmission; (2) every susceptible individual can remember the cumulative pieces of non-redundant information that the individual received from his or her neighbors, leading to a non-Markovian contagion process. For appropriately depicting the LI characteristics, we propose a gate-like adoption probability involving two key ingredients: ‘on’ and ‘off’ thresholds, which denote the starting and turn-off point of behavior adoption regarding the ratio of adopted informants in neighbors. In addition, we develop an edge-based compartmental theory for qualitative validation. Numerical simulations and theoretical analyses demonstrate that LI effect prominently influences the final adoption size. In detail, given information transmission probability, there exists an optimal imitation capacity in terms of the ‘on’ threshold to maximize the final adoption size, and, with fixed ‘on’ threshold, greater ‘off’ threshold will increase the final adoption size more. Moreover, the variation of imitation capacity versus information transmission probability induces a crossover phenomenon of final adoption size, i.e. enhancing imitation capacity (corresponding to the increase of the ‘on’ threshold) causes phase transition of final adoption size transform from the second-order continuity to the first-order discontinuity, where a bifurcation occurs. Importantly, through further investigation, the above findings qualitatively remain unaffected by the heterogeneity level of the degree distribution.

The rest of this paper is organized as follows: In section 2, we propose a new model to take into account the characteristics of LI effect. In section 3, we make numerical simulations and discuss the LI characteristics in behavior spreading. In section 4, we give an edge-based compartmental theory to explain the numerical results. Finally, in section 5, we present conclusions.

## 2. Social contagion model with LI effect

For investigating the LI effect in social contagion, we here appropriately leverage the generalized Susceptible-Adopted-Recovered (SAR) model [25] to depict the behavior spreading in complex networks with  $N$  nodes and a degree distribution  $P(k)$ , where nodes represent individuals of population and the spreading process only happens between the linked neighboring nodes. At each time step each individual is in either a susceptible ( $S$ ), adopted ( $A$ ) or recovered ( $R$ ) status. An individual in the susceptible state has not adopted the behavior no matter whether he has received the information, in the adopted state has accepted the behavior and transmits the information to the susceptible individuals, and in the recovered state has abandoned the behavior and refuses to transmit the information again.

To describe the LI effect in social contagion, we conceive an gate-like adoption probability distribution function  $h(x, \alpha, \Delta)$ , defined as follows:

$$h(x, \alpha, \Delta) = \begin{cases} 0, & 0 \leq x < \alpha, \\ 1, & \alpha \leq x < \alpha + \Delta, \\ 0, & \alpha + \Delta \leq x \leq 1, \end{cases} \quad (1)$$

where  $x \in [0, 1]$  denotes the ratio of adopted informants to the individual neighbors, and  $\alpha$  and  $\Delta$  indicate the ‘on’ threshold and gate width respectively. Besides, the ‘on’ threshold  $\beta = \alpha + \Delta$ . The  $h(x, \alpha, \Delta)$  function is demonstrated in figure 1. In figure 1, the parameter  $\alpha$  represents the ‘on’ threshold, after which the behavior will be adopted with probability 1. The parameter  $\beta$  represents the ‘off’ threshold, after which the fraction of adopted informants will inversely cause the rejection to the behavior. Small  $\alpha$  means individual will more easily adopt the behavior when he or she has only received a small number of pieces of information from adopted neighbors, and vice versa. Great  $\beta$  can keep individual consistently in adopting the behavior even though there is a larger fraction of adopted informants. When given  $\alpha$ , the greater  $\Delta$  means greater  $\beta$ . The parameter  $\Delta$  can help us learn how the tolerance of the fraction from the ‘on’ threshold to the ‘off’ threshold influences the final adoption size.

The behavior spreading process with non-redundant memory and social reinforcement is:

- (i) We denote the initial seed fraction as  $\rho_0$ . The rest of the nodes stay in the susceptible state.
- (ii) Renewing the states of individuals leverages the synchronous updating method [9]. At each time step, every adopted individual will transmit the information to each of its susceptible neighbors independently, through a transmission

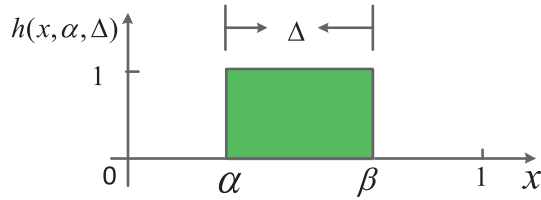


**Figure 1.** Schematic of gate-like behavior adoption probability  $h(x, \alpha, \Delta)$ , where  $x$  denotes the fraction of adopted informants in neighbors. In behalf of the critical fraction of adopted informants,  $\alpha$  represents the ‘on’ threshold, after which the behavior will be adopted with probability 1. The parameter  $\beta$  represents the ‘off’ threshold, after which the fraction of adopted informants will inversely cause the rejection to the behavior. Besides,  $\Delta = \beta - \alpha$  indicates the gate width, the greater value of which implies the behavior adoption will persist in more fraction of adopted informants.

probability  $\lambda$ . Once the information is successfully transmitted to a neighbor, the cumulative number  $m$  of received information of this neighbor will add one, i.e.  $m \rightarrow m + 1$ . In our model, alongside the same edge, retransmission of the same information will not increase the credibility and legitimacy of the behavior. Thus, with respect to non-redundant memory, an edge that has transmitted the information successfully will never transmit the same information again.

- (iii) At a time step  $t$ , if the degree of a susceptible individual is  $k$ , and he or she has received  $m$  pieces of information from distinct neighbors by time  $t$ , the probability for the susceptible individual to adopt the relative behavior is  $h(m/k, \alpha, \Delta)$  (referring to equation (1)). Only when the fraction  $m/k \in [\alpha, \beta)$ , the adoption will occur. At the same time step, each adopted individual will refuse to transmit the information again and enter into the recovered status with probability  $\gamma$ .
- (iv) The spreading will repeat until there is no adopted individual left.

### 3. Numerical results

In numerical simulations, we respectively apply the Erdős–Rényi (ER) [42] and uncorrelated configuration Scale-Free (SF) [43] random network to the study of the behavior spreading process, with the network size  $N = 10^4$  and the average degree  $\langle k \rangle = 10$ . Through extensive numerical simulations, we find that  $\gamma$  does not qualitatively affect the phenomenon. We thus set  $\gamma = 1.0$  in the main text. The relative variance  $v_R$  [44] is introduced numerically to determine the size-dependent critical values  $\lambda_c^I$  as follows

$$v_R = \frac{\langle (R(\infty) - \langle R(\infty) \rangle)^2 \rangle}{\langle R(\infty) \rangle^2}, \tag{2}$$

where  $\langle \dots \rangle$  is the ensemble average. The value of  $v_R$  shows the peaks (indicating phase transitions) of  $R(\infty)$  at the critical point when a dynamical parameter is varied. Thus

we know that the critical point  $\lambda_c^I$  corresponds to the maximum  $v_R$  under different values of  $\lambda$ .

To begin with the study in ER network, we investigate the time-evolution of the behavior spreading with the LI effect in figure 2 with  $\lambda = 0.8, \alpha = 0.1, \Delta = 0.2$ . Figure 2(a) shows the time-evolution of node density respectively in the susceptible status  $S(t)$ , the adopted status  $A(t)$ , and the recovered status  $R(t)$ . In detail, the density of the susceptible (recovered) nodes decreases (increases) with time and arrives at a certain value at the steady time. The density of the adopted initially increases, and reaches the peak at time step 9.

Furthermore, we analyze the average of degree of newly adopted individuals with time. Let us focus on the alteration of the adopted status and, at each time step in figure 2(b), see the average degree of newly adopted nodes [45] as follows

$$\langle k_A(t) \rangle = \frac{\sum_k k [I_k(t) - I_k(t-1)]}{I(t) - I(t-1)}. \quad (3)$$

Here,  $I_k(t)$  and  $I(t)$  separately denote the number of adopted nodes in degree class  $k$  and in all degree classes at time  $t$ . Besides, we meanwhile care about the inverse participation ratio [45]

$$Y_2(t) = \sum_k \left[ \frac{I_k(t)}{I(t)} \right]^2 \quad (4)$$

at each time step in figure 2(c). From the above two metrics, we find behavior spreading presents hierarchical characteristics. Totally speaking of the hierarchical spreading, adoption firstly exists in large degree classes, then progressively influences lower degree classes, and finally induces the capillary invasion to the lowest degree classes which have a larger number of nodes and thus exhibit a larger weight.

In detail, at time step 1, the only randomly selected seed holds the degree around 10 corresponding to the average degree of the ER network, since the individuals will adopt the behavior only when they receive one piece of information. From time step 2,  $\langle k_A(t) \rangle$  slowly increases initially, then reaches the peak, and decreases until the last time step. We zoom in the process at the typical time step 2 and 9, and expose the degree distribution of adopted nodes. We find that at the beginning of the spreading the degrees of adopted nodes are small, even less than the network average degree 10 (see the lower left inset at time step 2). Gradually, when the neighboring adopted nodes become many, some nodes with larger degree (see the upper right inset at time step 9) have the chance to adopt the behavior. After the hub nodes adopt the behavior, the rest very small-degree susceptible nodes can contact the behavior information and continue to adopt the behavior (see the downward curve after time step 9). The above hierarchical spreading phenomenon also can be detected in figure 2(c).

Moreover, the figures 2(d)–(f) correspondingly provide the snapshots of the time-evolution under LI effect. We can clearly see that at time step 1, there is only one seed in figure 2(d), then at time step 2 of figure 2(e), several susceptible nodes around the seed turn into the adopted and the seed enters into the recovered status, and at time step 9 so many nodes becomes adopted and recovered and few nodes remain susceptible in figure 2(f).

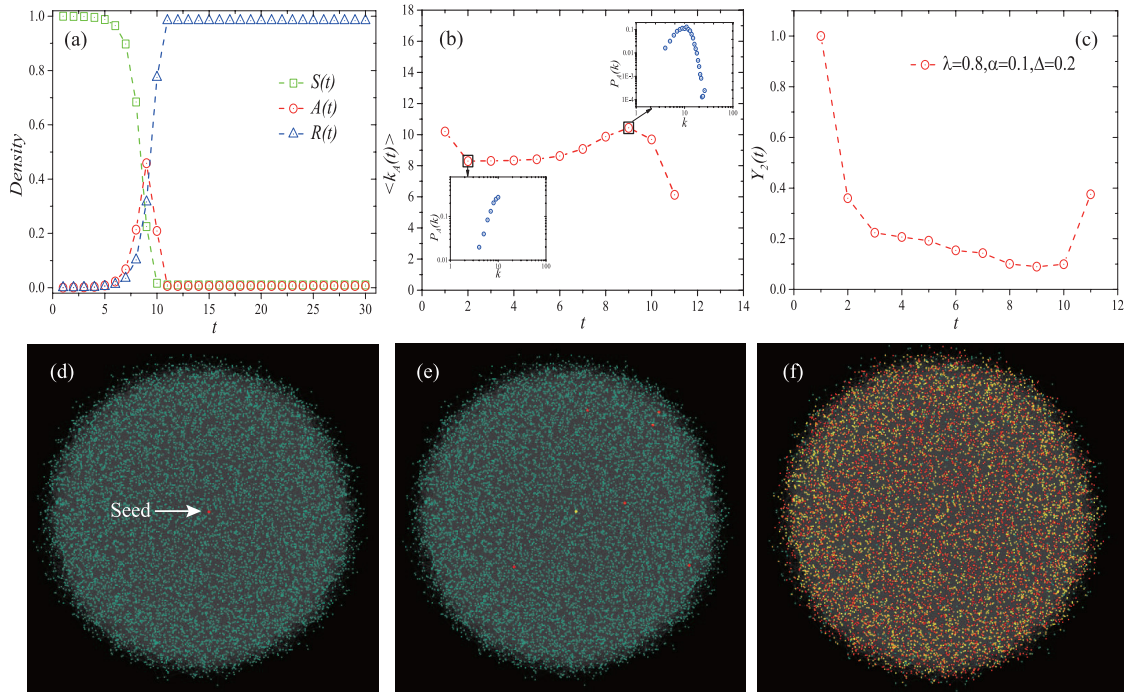


**Figure 2.** Demonstration of time-evolution characterized by LI effect in ER network with  $\lambda = 0.8, \alpha = 0.1, \Delta = 0.2$ . Here network size  $N = 10^4$ , average degree  $\langle k \rangle = 10$ , vaccination probability  $\gamma = 1.0$ , and seed fraction  $\rho_0 = 1/N$ . (a) The density time-evolution of three states, the susceptible  $S(t)$ , the adopted  $A(t)$ , and the recovered  $R(t)$ . (b) Average degree of the newly adopted nodes at time  $t$  [45]. Here, the bottom left and upper right insets represent the degree distribution of adopted nodes at time 2 and 9, respectively. (c) The inverse participation ratio [45]. (d)–(f) Snapshots of node time-evolution in three statuses at time 1, 2, and 9, with the susceptible node in green, the adopted node in red, and the recovered node in yellow.

Besides the time-evolution, we further investigate the phase transition of the final adoption size  $R(\infty)$  versus  $\lambda$  under LI effect, and demonstrate the results in figure 3. Symbols and dash lines indicate the numerical simulations and the theoretical solutions, respectively. When the ‘on’ threshold  $\alpha$  is very small, such as 0.06 in figures 3(a) and (b), the final adoption size  $R(\infty)$  increases continuously with  $\lambda$ , which means a second-order phase transition in the system with the increase of  $\alpha$ , such as 0.1. In figures 3(c) and (d), the final adoption size  $R(\infty)$  increases discontinuously with the increase of  $\lambda$  as a first-order phase transition. The transformation of phase transition here is called the crossover phenomenon [46], which can be further highlighted by contrasting (a)–(c) or (b)–(d) with different  $\alpha$ . In addition, the numerical simulations agree with the theoretical solutions very well.

To intuitively understand the abrupt increase of  $R(\infty)$  as  $\lambda$  passes through a critical point, we focus on the individuals in the subcritical state. In such state, an individual  $u$  with degree  $k$  has received  $m$  pieces of information with precisely one piece less than the adoption threshold, i.e.  $m = \lceil k\alpha \rceil - 1$ , and has not yet adopted the behavior. Say at the same time,  $u$  has received information from his or her neighbors but neighbor  $v$ . Now

assume that  $v$  has adopted the behavior and transmits the information to  $u$  successfully, leading to the behavior adoption by  $u$ . In turn,  $u$  will transmit the information to his or her susceptible neighbors with probability  $\lambda$ . As a result, some neighbors in the subcritical state adopt the behavior. The process will repeat step by step, cumulatively resulting in an avalanche of behavior adoption. If there are considerably large number of individuals in the subcritical state, a tiny increase in the number of adopted individuals, e.g. by rising  $\lambda$  a little, may induce a sudden and large number of subcritical individuals to adopt the behavior, causing a discontinuous ‘jump’ in the value of  $R(\infty)$ .

The above intuitive explanation is further proved by numerical simulations and theoretical solutions in figures 3(e)–(h). The peak of subcritical  $\Phi(\infty)$  curve at the critical probability  $\lambda_c^I$  just points to the critical ‘jump’ point of  $R(\infty)$ . Noticeably, the peak values in figures 3(e) and (f) are much smaller than those in figures 3(g) and (h), implying that the quantities of subcritical individuals in figures 3(e) and (f) are less than in figures 3(g) and (h). The considerable difference in number of subcritical individuals leads to the crossover phenomenon from the continuity to the discontinuity in the phase transition.

The critical point  $\lambda_c^I$  can be numerically acquired by the relative variance  $v_R$  in figures 3(i)–(l). According to equation (2), we can get the  $v_R$  curve versus  $\lambda$  and the peak just corresponds to critical point  $\lambda_c^I$ . The  $\lambda_c^I$  in figures 3(i)–(l) coincide with the corresponding peaks in figures 3(e) and (f) very well.

We explore the effects of seed fraction  $\rho_0$  on the final adoption size  $R(\infty)$  versus spreading probability  $\lambda$  in figure 4. We find that  $R(\infty)$  increases with  $\rho_0$ . Importantly, we note that  $R(\infty)$  increases continuously with  $\lambda$  for large values of  $\rho_0$ . Our theory can well predict the above phenomena.

We further investigate the effects of  $\alpha$  on  $R(\infty)$  in figure 5. We find that for a given  $\Delta$ , there always exists an optimal  $\alpha$  maximizing the final adoption size  $R(\infty)$  (see the peaks in subgraphs). We call such phenomenon of optimal  $\alpha$  under LI effect as the optimal imitation capacity. Since the network structure is fixed, when the ‘on’ threshold  $\alpha$  is small, many individuals with small number  $k$  of neighbors can easily adopt the behavior after receiving  $m$  pieces of information, but many individuals with a relatively great  $k$  of neighbors will abandon the behavior because the given gate width  $\Delta$  accordingly produces a small ‘off’ threshold. Besides, increasing  $\alpha$  is equivalent to moving the adoption window towards the right and enlarging the ‘off’ threshold  $\beta$ , causing some individuals with smaller number of neighbors fail to adopt the behavior. At the same time, some other individuals with greater number of neighbors will meet the condition to adopt the behavior. If the number of newly satisfied individuals is more than the number of the individuals losing chance, the final adoption size  $R(\infty)$  will continue to increase until the variation attains balance. At this time, the  $R(\infty)$  reaches the peak and  $\alpha$  arrives at the optimal. Then proceeding to increase  $\alpha$  will cause more individuals lose chance than the newly satisfied individuals. As a result  $R(\infty)$  ever-lastingly declines. Furthermore, at certain  $\alpha$  when all individuals lose the chance to adopt the behavior, an abrupt ‘fall’ of  $R(\infty)$  will happen directly to a value of zero. Besides, through comparison between figures 5(a)–(c), we also uncover, given  $\alpha$ , larger  $\Delta$  can enlarge the final adoption size  $R(\infty)$ , which is also unfolded in figure 6.

In figure 6, we pay attention to the dependance of  $R(\infty)$  on the gate width  $\Delta$ , based on the combinations of  $\lambda = 0.1, 0.2, 0.5$  and  $\alpha = 0.01, 0.06, 0.09$ . Here we find for a given

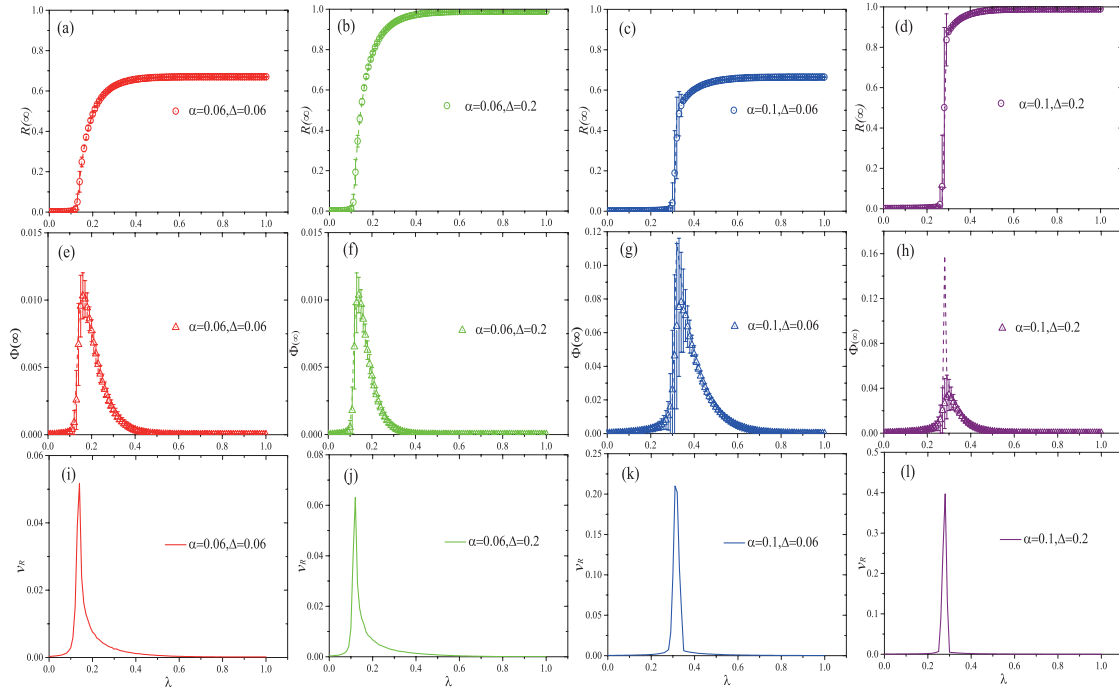


**Figure 3.** Demonstration of the crossover phase transition of the final adoption size  $R(\infty)$  versus  $\lambda$  triggered by the ‘on’ threshold  $\alpha$  of LI effect, related to  $\alpha = 0.06, 0.1$  and  $\Delta = 0.06, 0.2$  in ER network. Here network size  $N = 10^4$ , average degree  $\langle k \rangle = 10$ ,  $\gamma = 1$ , and seed fraction  $\rho_0 = 1/N$ . Symbols and dash lines indicate the numerical simulations and the theoretical solutions, respectively. (a)–(d) Crossover phase transition of  $R(\infty)$  versus  $\lambda$ , corresponding to the circle symbol. (e)–(h) The ratio  $\Phi(\lceil k\alpha \rceil - 1, \infty)$  of individuals in the subcritical state versus  $\lambda$ , corresponding to the up triangle symbol. (i)–(l) The relative variance  $v_R$  versus  $\lambda$ , corresponding to the solid line.

$\alpha$ , increasing  $\Delta$  can enlarge the final adoption size  $R(\infty)$ . The reason is: When given  $\alpha$ , widening  $\Delta$  will increase the ‘off’ threshold, making more and more individuals with different numbers  $k$  of neighbors satisfy the adoption ratio when they have received  $m$  pieces of information; At the same time, less individuals lose the adoption chance or abandon. At certain  $\Delta$  when all individuals can satisfy the adoption condition, the final adoption size  $R(\infty)$  will reach the maximum and keep the same till the end. Through horizontal comparison from figures 6(a)–(c), we find increasing  $\alpha$  holistically reduces the  $R(\infty)$ , especially when the  $\lambda$  is small (see figure 6(c)). At this time, more individuals cannot meet the adoption condition with enough ratio of adopted informants. As a result, the smaller transmission probability causes more difficulty in information transmission and worsens the above situation, exhibiting the consistent phenomenon with figure 5.

Besides the research on the ER network, we also investigate the LI effect in SF network with network size  $N = 10^4$  and average degree  $\langle k \rangle = 10$ . The minimum degree is 4 and the cutoff for the maximum degree is 100. The uncorrelated networks are generated with the power-law degree distribution  $P(k) \sim k^{-v}$  ( $v$  being the degree exponent) according to the method in [43]. Under LI effect, an individual will adopt the behavior

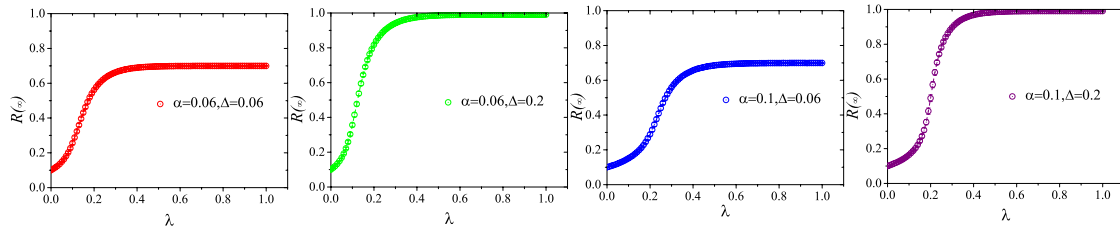


**Figure 4.** Dependence of the final adoption size  $R(\infty)$  on  $\lambda$  with  $\rho_0 = 0.1$  triggered by the ‘on’ threshold  $\alpha$  of LI effect, related to  $\alpha = 0.06, 0.1$  and  $\Delta = 0.06, 0.2$  in ER network. Here network size  $N = 10^4$ , average degree  $\langle k \rangle = 10$  and  $\gamma = 1$ . Symbols and dashed lines indicate the numerical simulations and the theoretical solutions, respectively.

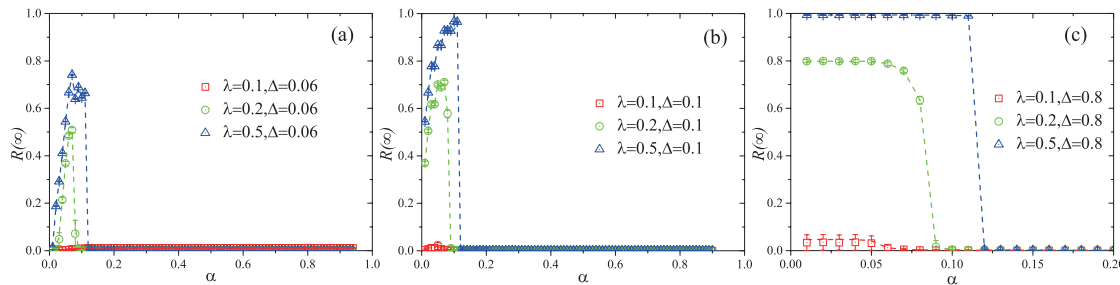


**Figure 5.** Demonstration of dependence of the final adoption size  $R(\infty)$  on the ‘on’ threshold  $\alpha$ , concerning  $\lambda = 0.1, 0.2, 0.5$  and  $\Delta = 0.06, 0.1, 0.8$ , characterized by LI effect in ER network. Here network size  $N = 10^4$ , average degree  $\langle k \rangle = 10$ ,  $\gamma = 1$ , and seed fraction  $\rho_0 = 1/N$ . Symbols and dashed lines indicate the numerical simulations and the theoretical solutions, respectively.

only if he or she has successfully received  $m = \lceil k\alpha \rceil$  pieces of information, with  $k$  and  $\alpha$  denoting the number of neighbors and ‘on’ threshold. In SF network, small  $v$  means large heterogeneity level of degree distribution and vice versa. In figure 7, we provide the  $R(\infty)$  curves versus  $\lambda$  to uncover the influence from the heterogeneity level of degree distribution, in terms of different degree exponent  $v = 2.1, 3$ , and 4. We find that increasing the heterogeneity of network structure (by reducing the value of the degree exponent  $v$ ) will not affect the crossover phenomenon of phase transition. In detail, when the ‘on’ threshold is very small, e.g.  $\alpha = 0.01$  in (a) and (b) with  $\Delta = 0.05$  and 0.5, no matter what the exponent degree  $v$  is,  $R(\infty)$  versus  $\lambda$  always exhibits the continuous second-order phase transition. When the ‘on’ threshold becomes large, e.g.  $\alpha = 0.1$  in (c) and (d) corresponding to  $\Delta = 0.05$  and 0.5,  $R(\infty)$  versus  $\lambda$  still presents the discontinuous first-order phase transition regardless of  $v$ . The result can be qualitatively explained as follows: Given gate width  $\Delta$  and small ‘on’ threshold  $\alpha$ , when spreading probability  $\lambda$  is small, under LI effect, only individuals with small number of neighbors (i.e. with smaller degree  $k$ ) can easily receive enough pieces of behavior information and thus adopt the behavior. With the increase of  $\lambda$ , many individuals with larger number of neighbors also gradually become easy to receive enough pieces of information and then adopt the behavior. Under such condition, few individuals in subcritical state will be cumulated and adopt the behavior at once. Therefore, for small value of  $v$ ,  $R(\infty)$  versus  $\lambda$  exhibits the continuous first-order phase transition.

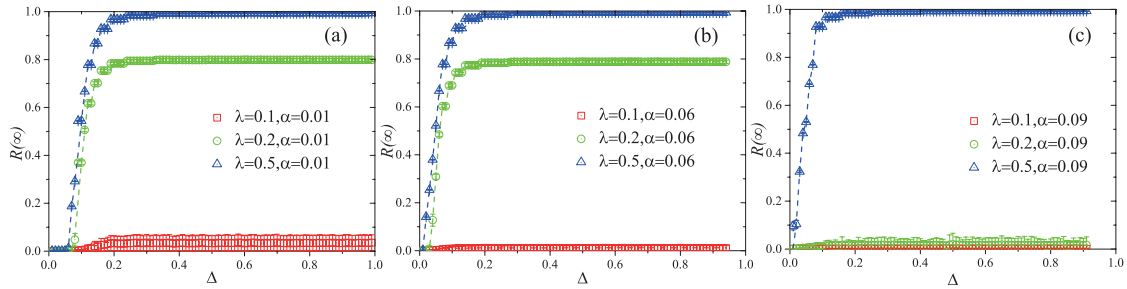


**Figure 6.** Demonstration of dependence of the final adoption size  $R(\infty)$  on the gate width  $\Delta$ , related to  $\lambda = 0.1, 0.2, 0.5$  and  $\alpha = 0.01, 0.06, 0.09$ , characterized by LI effect in ER network. Here network size  $N = 10^4$ , average degree  $\langle k \rangle = 10$ ,  $\gamma = 1$ , and seed fraction  $\rho_0 = 1/N$ . Symbols and dash lines indicate the numerical simulations and the theoretical solutions, respectively.

In contrast, given gate width  $\Delta$  and large ‘on’ threshold  $\alpha$ , the adopt condition of  $m = \lceil k\alpha \rceil$  pieces of information become more difficult to be met for the same degree  $k$ . At this time, small  $\lambda$  will aggravates the difficulty of adoption. With the increase of  $\lambda$ , because of the large ‘on’ threshold  $\alpha$ , more and more individuals enter into the subcritical state but have not adopted the behavior. At certain  $\lambda$ , the massively cumulated individuals suddenly adopt the behavior at once, causing the abrupt ‘jump’ of  $R(\infty)$  and bringing in the discontinuous second-order phase transition. In a word, under LI effect, heterogeneity of degree distribution, corresponding to  $v$ , just influences the size of  $R(\infty)$  instead of pattern of phase transition.

#### 4. Theoretical analysis based on edge-based compartmental theory

To unveil the essence, we proceed to provide a theoretical analysis to explain the behavior spreading under LI effect. We develop a generalized edge-based compartmental theory based on [25, 26, 47, 48]. For convenience, we define mathematical symbols  $S(t)$ ,  $A(t)$ , and  $R(t)$  as the fraction of individuals in the susceptible, adopted, and recovered states at time step  $t$ . Especially,  $R(\infty)$  represents the steady state when  $t \rightarrow \infty$ .

We suppose individual  $u$  in the cavity state [49], which can receive behavior information from adopted neighbors but cannot propagate the information to neighbors. We define  $\theta(t)$  as the probability that individual  $v$  by time  $t$  has not transmitted the behavior information to individual  $u$  alongside a randomly selected edge. Thus, by time  $t$ , an individual  $u$  with degree  $k$  has received  $m$  pieces of information from different neighbors with probability

$$\phi_m(k, t) = \binom{k}{m} [\theta(t)]^{k-m} [1 - \theta(t)]^m. \quad (5)$$

The probability that individual  $u$  with degree  $k$  has received  $m$  pieces of information but keeps susceptible is  $\prod_{j=0}^m [1 - h(\frac{j}{k}, \alpha, \Delta)]$ . Furthermore, we can obtain the probability that such individual  $u$  by time  $t$  is still in susceptible state as

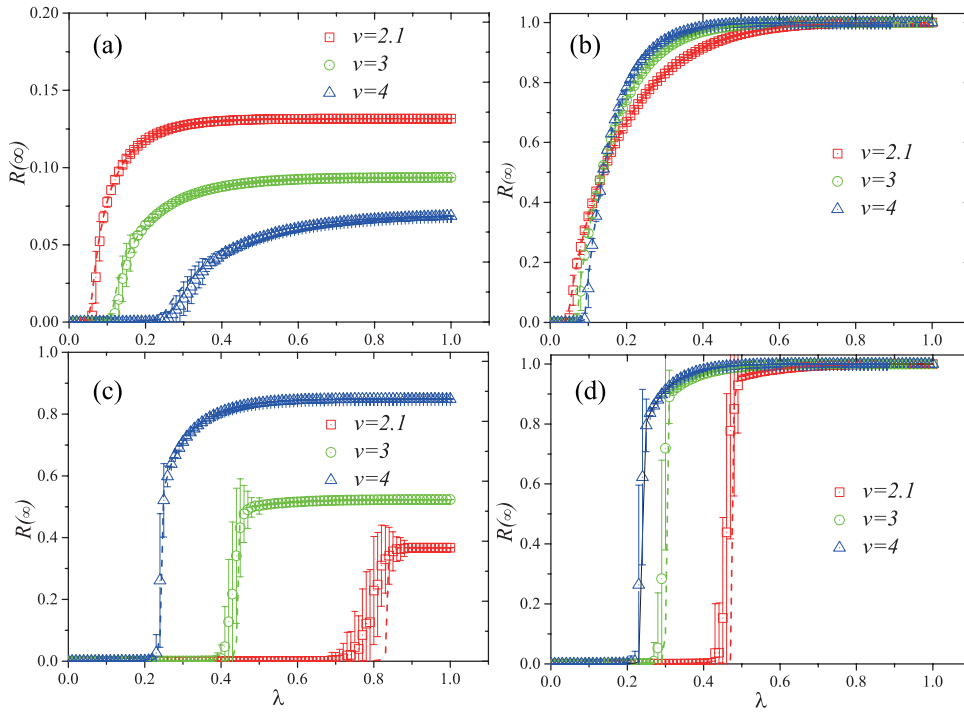


**Figure 7.** Demonstration of the dependence of  $R(\infty)$  versus  $\lambda$  on SF network, under exponent  $v = 2.1, 3, 4$ , with  $\alpha = 0.01, \Delta = 0.05$  in (a),  $\alpha = 0.01, \Delta = 0.5$  in (b),  $\alpha = 0.1, \Delta = 0.05$  in (c), and  $\alpha = 0.1, \Delta = 0.5$  in (d). Network size  $N = 10^4$ , average degree  $\langle k \rangle = 10$ ,  $\gamma = 1$ , and seed fraction  $\rho_0 = 1/N$ . The minimum degree is 4 and the cutoff for the maximum degree is 100. Symbols and dashed lines indicate the numerical simulations and the theoretical solutions, respectively.

$$\begin{aligned}
 S(k, t) &= \sum_{m=0}^k \phi_m(k, t) \prod_{j=0}^m [1 - h(\frac{j}{k}, \alpha, \Delta)] \\
 &= \sum_{m=0}^{\lfloor bk \rfloor} \phi_m(k, t).
 \end{aligned}
 \tag{6}$$

Traversing all possible degrees  $k$ , we achieve the whole ratio that susceptible individuals account for as

$$S(t) = \sum_k P(k) S(k, t).
 \tag{7}$$

where  $P(k)$  is the degree distribution.

Analogously, the fraction of individuals with  $m$  pieces of information at time  $t$  is

$$\Phi(m, t) = \sum_{k=0}^{\infty} P(k) \phi_m(k, t).
 \tag{8}$$

Since neighbor  $v$  of individual  $u$  possibly stays in either susceptible, adopted, or recovered status,  $\theta(t)$  can be represented as

$$\theta(t) = \xi_S(t) + \xi_A(t) + \xi_R(t), \tag{9}$$

where  $\xi_S(t)$  [ $\xi_A(t)$ ,  $\xi_R(t)$ ] is the probability that neighbor  $v$  of individual  $u$  is in the susceptible (adopted, recovered) state and has not transmitted the behavioral information to  $u$  by time  $t$ .

At the beginning, individual  $v$  with degree  $k'$  is susceptible, and cannot transmit behavior information to  $u$ . He or she can receive information from the other  $k' - 1$  neighbors except susceptible  $u$ . Thus, individual  $v$  by time  $t$  has received  $m$  units of information with probability

$$\phi_m(k' - 1, t) = \binom{k' - 1}{m} [\theta(t)]^{k' - m - 1} [1 - \theta(t)]^m. \tag{10}$$

With all possible values of  $m$ , individual  $v$  of degree  $k'$  remains susceptible with probability

$$\begin{aligned} \Theta(k', t) &= \sum_{m=0}^{k'-1} \phi_m(k' - 1, t) \prod_{j=0}^m [1 - h(\frac{j}{k'}, \alpha, \Delta)] \\ &= \sum_{m=0}^{\lfloor \alpha k' \rfloor} \phi_m(k' - 1, t) \prod_{j=0}^m [1 - h(\frac{j}{k'}, \alpha, \Delta)] \\ &\quad + \sum_{m=\lfloor \alpha k' \rfloor}^{k'-1} \phi_m(k' - 1, t) \prod_{j=0}^m [1 - h(\frac{j}{k'}, \alpha, \Delta)] \\ &= \sum_{m=0}^{\lfloor \alpha k' \rfloor} \phi_m(k' - 1, t). \end{aligned} \tag{11}$$

In an uncorrelated network, an edge connects an individual of degree  $k'$  with probability  $k'P(k')/\langle k \rangle$ , where  $\langle k \rangle$  is the average degree. We obtain

$$\xi_S(t) = \sum_{k'} \frac{k'P(k')}{\langle k \rangle} \Theta(k', t). \tag{12}$$

If an individual in adopted status transmits behavior information through an edge with probability  $\lambda$ ,  $\theta(t)$  will reduce the fraction  $\lambda\xi_A(t)$ , i.e.

$$\frac{d\theta(t)}{dt} = -\lambda\xi_A(t). \tag{13}$$

If an adopted individual does not transmit the behavior information through any edge with probability  $1 - \lambda$  but turns into the recovered state with probability  $\gamma$ ,  $\xi_R(t)$  will consequently increase a fraction

$$\frac{d\xi_R(t)}{dt} = \gamma(1 - \lambda)\xi_A(t). \tag{14}$$

Using equations (13) and (14), and the initial conditions of  $\theta(0) = 1$  and  $\xi_R(0) = 0$ , we get

$$\xi_R(t) = \frac{\gamma[1 - \theta(t)](1 - \lambda)}{\lambda}. \tag{15}$$

Substituting  $\xi_S(t)$ ,  $\xi_A(t)$  and  $\xi_R(t)$  of equation (9) into equations (12), (13) and (15), respectively, we acquire the time evolution of  $\theta(t)$  as

$$\frac{d\theta(t)}{dt} = -\lambda[\theta(t) - \sum_{k'} \frac{k'P(k')}{\langle k \rangle} \Theta(k', t)] + \gamma[1 - \theta(t)](1 - \lambda). \tag{16}$$

At each time step  $t$ , some susceptible individuals adopt the behavior and some adopted individuals move into the recovered state. Note that the growth of  $A(t)$  is equivalent to the decrease of  $S(t)$  minus the fraction of adopted individuals that with probability  $\gamma$  enter into the recovered state. Thus the time evolution of  $A(t)$  is

$$\begin{aligned} \frac{dA(t)}{dt} &= -\frac{dS(t)}{dt} - \gamma A(t) \\ &= -\sum_k P(k) \frac{dS(k, t)}{dt} - \gamma A(t). \end{aligned} \tag{17}$$

The time evolution of  $R(t)$  is

$$\frac{dR(t)}{dt} = \gamma A(t). \tag{18}$$

Equations (5)–(7), (16) and (17) describe social contagion in terms of LI effect, and can determine the fraction of each state at arbitrary time step. When  $t \rightarrow \infty$ , we find the final adoption size  $R(\infty)$ .

In the final state, we find that

$$\theta(\infty) = \sum_{k'} \frac{k'P(k')}{\langle k \rangle} \Theta(k', \infty) + \frac{\gamma[1 - \theta(\infty)](1 - \lambda)}{\lambda}. \tag{19}$$

Note that  $\theta(t)$  diminishes with  $t$  when adopted individuals continually transmit the behavior information to neighbors. Thus in the case of more than one stable fixed point in equation (19) only the maximum stable fixed point is physically meaningful. Inserting this value into equations (5)–(7) gives us the steady value of the susceptible density  $S(\infty)$  and the final behavior adoption size  $R(\infty)$ .

At the critical point, the equation

$$g(\theta, \alpha, \Delta, \gamma, \lambda) = \sum_{k'=1}^{N-1} \frac{k'P(k')}{\langle k \rangle} \Theta(k', \infty) + \frac{\gamma[1 - \theta(\infty)](1 - \lambda)}{\lambda} - \theta(\infty) \tag{20}$$

is tangent to the horizontal axis at  $\theta(\infty) = 1$ . Thus the critical condition of the general social contagion model satisfies

$$\left. \frac{dg}{d\theta(\infty)} \right|_{\theta(\infty)=1} = 0. \tag{21}$$

From equation (21), the continuous critical information transmission probability can be achieved as

$$\lambda_c^I = \frac{\gamma}{\Gamma + \gamma - 1}, \quad (22)$$

where

$$\Gamma = \sum_{k'} \frac{k' P(k')}{\langle k \rangle} \frac{d\Theta(k', \theta(\infty))}{d\theta(\infty)} \Big|_{\theta(\infty)=1}.$$

From equation (21), we can obtain the critical condition. Since initially a vanishingly small fraction of seeds are randomly selected and all individuals conform to the consistent adoption probability distribution  $h(x, \alpha, \Delta)$ , equation (19) possesses one trivial solution,  $\theta(\infty) = 1$ . At the critical point, the function  $g[\theta, \alpha, \Delta, \gamma, \lambda]$  is tangent to horizontal axis at  $\theta(\infty) = 1$ . For  $\alpha k < 1$  and  $\lceil k\alpha \rceil = 0$ , leveraging equation (19)–(22), we can get the continuous critical transmission probability as

$$\lambda_c^{II} = \frac{\gamma \langle k \rangle}{\langle k^2 \rangle - 2\langle k \rangle + \gamma \langle k \rangle}, \quad (23)$$

which exhibits the same form as the one of epidemic outbreak threshold. For  $\alpha k \geq 1$  and  $\lceil k\alpha \rceil > 0$ , the function  $g[\theta, \alpha, \Delta, \gamma, \lambda]$  can never be tangent to the horizontal axis, implying that a vanishingly small fraction of initial seeds cannot induce a finite fraction of individuals to adopt the behavior.

We mainly care about how the LI effect under non-redundant memory influences the dependence of  $R(\infty)$  on the transmission probability  $\lambda$ , which can be elucidated by the situation of roots from equation (19). Numerically solving equations (19)–(22), we find  $\lambda_c^I$  is associated with adoption probability  $h(x, \alpha, \Delta)$ , recovery probability  $\gamma$ , degree distribution  $P(k)$ , and average degree  $\langle k \rangle$ . When given all the parameters except  $\lambda$ , we can more easily analyze the dependence. If equation (19) has only two roots for different values of  $\lambda$ , as in figure 8(a) with  $\alpha = 0.06$ ,  $\Delta = 0.2$ , the trivial solution of equation (19) is  $\theta(\infty) = 1$  and there is no global behavior adoption.  $R(\infty)$  will increase continuously.

In the second scenario, if the number of roots of equation (19) is determined by  $\lambda$ , there will appear three roots and only the largest solution is valid, showing a saddle-node bifurcation [50], as shown in figure 8(b). Equation (19) possess a non-trivial solution  $\theta(\infty) < 1$ . Changing  $\lambda$  induces the physically meaningful stable solution of  $\theta(\infty)$  to jump to an alternate value. A discontinuous growth pattern of  $R(\infty)$  with  $\lambda$  occurs. In figure 8(b) with  $\alpha = 0.1$ , for different values of  $\lambda$ , the function  $g[\theta, \alpha, \Delta, \gamma, \lambda]$  is tangent to the horizontal axis at  $\lambda_c^I = 0.232$ . When  $\lambda > \lambda_c^I$ , if there are three fixed points in equation (19), e.g.  $\lambda = 0.24$ , the largest is the solution. When  $\lambda = \lambda_c^I$ , the tangent point is the solution. When  $\lambda < \lambda_c^I$ , e.g.  $\lambda = 0.22$ , the only fixed point is the solution of equation (19), which abruptly drops to a small value from a large value at  $\lambda = \lambda_c^I$  and results in a discontinuous change in  $R(\infty)$ .

In addition, for comparison with numerical simulations, based on the above edge-based compartmental theory and theoretical equations, we compute the theoretical solutions and, at the same time, plot the theoretical curves in figures 3–7, correspondingly. We can find the theoretical solutions (denoted by the dash lines) coincide with numerical simulations (denoted by the symbols) very well.

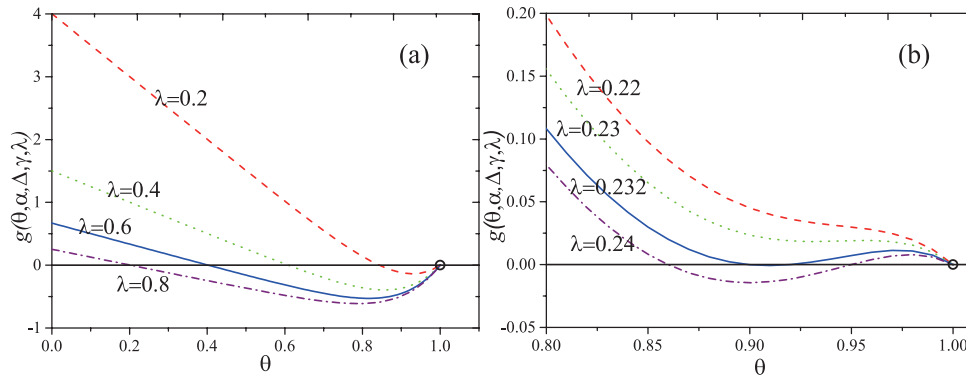


**Figure 8.** Demonstration of graphical solutions of equation (20) for with  $\alpha = 0.06$ ,  $\Delta = 0.2$  in (a) and  $\alpha = 0.1$ ,  $\Delta = 0.2$  in (b). The horizontal axis are colored black and the tangent points are denoted as black dots.

## 5. Conclusions

In this paper, based on the social contagion model with non-redundant memory, we have investigated an interesting LI effect, in which individual will adopt an behavior via imitating adopted informants in his neighbors up to a point that they lose the drive to continuously adopt. Correspondingly, we propose a gate-like adoption probability distribution consisting of the ‘on’ and ‘off’ thresholds to match the LI effect. Besides, for convenience of investigation, we further introduce the gate width variable equal to the ‘off’ threshold minus the ‘on’ threshold. Moreover, we novelly explore such effect with social reinforcement based on non-Markovian model.

Through extensive numerical simulations, we analyze the above effect in different aspects. We first examine the time-evolution process of the behavior spreading in LI effect and point out the hierarchical adoption from the nodes with small degree to the nodes with large degree, especially the hubs, then to a great many nodes with the smallest degrees. Moreover, we focus on the dependence of the final adoption size on the transmission probability, ‘on’ threshold and the gate width (indirectly representing the ‘off’ threshold). We discover that the small and large values of ‘on’ threshold respectively result in the continuous first-order and the discontinuous second-order phase transition of the final adoption size versus the transmission probability. When paying attention to the dependence on the ‘on’ threshold, given gate width and changing the value of the ‘on’ threshold, there exists an optimal ‘on’ threshold maximizing the final adoption size. We call such phenomenon as optimal imitation capacity in LI effect. Meanwhile, we discover great gate width can enlarge the final adoption size. At last, we find the above phenomena qualitatively are unaffected by different hierarchical level of degree distribution.

For quantitatively analyzing the essence of the LI effect, we tender an edge-based compartmental theory, under which we build the time-evolution rules and unveil the intrinsic mechanism of the crossover phase transition based on the analysis of function roots. We also provide the theoretical solutions for comparison with the numerical simulations. Generally, the numerical simulations and the theoretical analyses agree very well.

Moreover, the developed research on LI effect can assist in better understanding social behavioral information contagion, e.g. users' purchase behavior spreading, to help product marketing, new fashion prediction, new technology recommendation. The effects of network structure on our model need to be investigated, such as clustering coefficient, degree correlation, community structure, multiplex network structure, temporal network structure. Our results expand our understanding of phenomena in phase transitions and may provide new insights into spreading dynamics. In our current era of big data, there exist many challenging issues associated with social contagions that need to be addressed. For example, using real data to verify the effectiveness of our proposed social contagion. Our model may shed some light on studying the general minority games.

## Acknowledgments

This work was supported by the National Natural Science Foundation of China (Nos. 61602048, 61471060, 61673086), the Fundamental Research Funds for the Central Universities (Nos. 2017RC09, YJ201830, ZYGX2016J058), and the China Postdoctoral Science Foundation (CPSF) (No. 2018M631073).

## References

- [1] Watts D J and Dodds P S 2007 Influentials, networks, and public opinion formation *J. Consci. Res.* **34** 441–58
- [2] Castellano C, Fortunato S and Fortunato S 2009 Statistical physics of social dynamics *Rev. Mod. Phys.* **81** 591
- [3] Pastor-Satorras R and Vespignani A 2001 Epidemic spreading in scale-free networks *Phys. Rev. Lett.* **86** 3200
- [4] Wang W, Tang M, Yang H, Do Y, Lai Y C and Lee G W 2014 Asymmetrically interacting spreading dynamics on complex layered networks *Sci. Rep.* **4** 5097
- [5] Qi H K, Liu L D and Meng X Z 2017 Dynamics of a nonautonomous stochastic SIS epidemic model with double epidemic hypothesis *Complexity* **2017** 4861391
- [6] Malik H A M *et al* 2017 Robustness of dengue complex network under targeted versus random attack *Complexity* **2017** 2515928
- [7] Chen X L, Wang R J, Tang M, Cai S M, Stanley H E and Braunstein L A 2018 Suppressing epidemic spreading in multiplex networks with social-support *New J. Phys.* **20** 013007
- [8] Chen X L, Wang W, Cai S M, Stanley H E and Braunstein L A 2018 Optimal resource diffusion for suppressing disease spreading in multiplex networks *J. Stat. Mech.* **053501**
- [9] Porter M A and Gleeson J P 2016 Dynamical Systems on Networks: a Tutorial, *Frontiers Applied Dynamical Systems: Reviews and Tutorials* (Heidelberg: Springer)
- [10] Watts D J 2002 A simple model of global cascades on random networks *Proc. Natl Acad. Sci. USA* **99** 5766–71
- [11] Chen X L, Yang C, Zhong L F and Tang M 2016 Crossover phenomena of percolation transition in evolution networks with hybrid attachment *Chaos* **26** 083114
- [12] Gleeson J P and Cahalane D J 2007 Seed size strongly affects cascades on random networks *Phys. Rev. E* **75** 056103
- [13] Dodds P S and Payne J L 2009 Analysis of a threshold model of social contagion on degree-correlated networks *Phys. Rev. E* **79** 066115
- [14] Gleeson J P 2008 Cascades on correlated and modular random networks *Phys. Rev. E* **77** 046117
- [15] Granovetter M 1973 The strength of weak ties *Am. J. Sociol.* **78** 1360–80
- [16] Centola D 2011 An experimental study of homophily in the adoption of health behavior *Science* **334** 1269–72
- [17] Karsai M *et al* 2016 Local cascades induced global contagion: how heterogeneous thresholds, exogenous effects, and unconcerned behaviour govern online adoption spreading *Sci. Rep.* **6** 27178
- [18] Gao L, Wang W, Pan L M, Tangand M and Zhang H F 2016 Effective information spreading based on local information in correlated networks *Sci. Rep.* **6** 38220

- [19] Liu X Y, Chao L and Zeng X P 2017 Online social network emergency public event information propagation and nonlinear mathematical modeling *Complexity* **2017** 5857372
- [20] Aral S, Muchnik L and Sundararajan A 2009 Distinguishing influence-based contagion from homophily-driven diffusion in dynamic networks *Proc. Natl Acad. Sci. USA* **106** 21544–9
- [21] Christakis N A and Fowler J H 2007 The spread of obesity in a large social network over 32 years *New Engl. J. Med.* **2007** 370
- [22] Barrat A, Barthélemy M and Vespignani A 2007 *Dynamical Processes on Complex Networks* (Cambridge: Cambridge University Press)
- [23] Dodds P S and Watts D J 2004 Universal behavior in a generalized model of contagion *Phys. Rev. Lett.* **92** 218701
- [24] Zheng M, Lü L and Zhao M 2013 Spreading in online social networks: the role of social reinforcement *Phys. Rev. E* **88** 012818
- [25] Wang W, Tang M, Zhang H F and Lai Y C 2015 Dynamics of social contagions with memory of nonredundant information *Phys. Rev. E* **92** 012820
- [26] Wang W, Shu P, Zhu Y X, Tang M and Zhang Y C 2015 Dynamics of social contagions with limited contact capacity *Chaos* **25** 103102
- [27] Wang W, Tang M, Shu P and Wang Z 2016 Dynamics of social contagions with heterogeneous adoption thresholds: crossover phenomena in phase transition *New J. Phys.* **18** 013029
- [28] Karampourniotis P D *et al* 2015 The impact of heterogeneous thresholds on social contagion with multiple initiators *PLoS One* **10** e0143020
- [29] Unicomb S, Iñiguez G and Karsai M 2018 Threshold driven contagion on weighted networks *Sci. Rep.* **8** 3094
- [30] Backlund V P, Saramäki J and Pan R K 2014 Effects of temporal correlations on cascades: threshold models on temporal networks *Phys. Rev. E* **89** 062815
- [31] Liu M X, Wang W, Liu Y, Tang M, Cai S M and Zhang H F 2017 Social contagions on time-varying community networks *Phys. Rev. E* **95** 052306
- [32] Wang W, Cai M and Zheng M 2017 Social contagions on correlated multiplex networks *Physica A* **499** 121
- [33] Wang W, Chen X L and Zhong L F 2018 Social contagions with heterogeneous credibility *Physica A* **503** 604
- [34] Leibenstein H 1976 *Inside the Firm: the Inefficiencies of Hierarchy* (Cambridge, MA: Harvard University Press)
- [35] Simmel G 1957 Fashion *Am. J. Sociol.* **62** 541–58
- [36] Granovetter M and Soong R 1986 Threshold models of interpersonal effects in consumer demand *J. Econ. Behav. Organ.* **7** 83–99
- [37] Dodds P S, Harris K D and Danforth C M 2013 Limited imitation contagion on random networks: chaos, universality, and unpredictability *Phys. Rev. Lett.* **110** 158701
- [38] Arthur W B 1994 Inductive reasoning and bounded rationality *Am. Econ. Rev.* **84** 406
- [39] Challet D, Marsili M and Zecchina R 2000 Statistical mechanics of systems with heterogeneous agents: minority games *Phys. Rev. Lett.* **84** 1824
- [40] Challet D, Marsili M and Zhang Y C 2001 Stylized facts of financial markets and market crashes in minority games *Physica A* **294** 514
- [41] Challet D, Marsili M and Zhang Y C 2013 *Minority Games: Interacting Agents in Financial Markets* (Oxford: Oxford University Press)
- [42] Erdős P and Rényi 1959 On random graphs *Publ. Math.* **6** 290–7
- [43] Catanzaro M, Boguná M and Pastor-Satorras R 2005 Generation of uncorrelated random scale-free networks *Phys. Rev. E* **71** 027103
- [44] Chen W, Schröder M and D'Souza M R 2014 Microtransition cascades to percolation *Phys. Rev. Lett.* **112** 155701
- [45] Barthélemy M, Barrat A, Pastor-Satorras R and Vespignani A 2004 Velocity and hierarchical spread of epidemic outbreaks in scale-free networks *Phys. Rev. Lett.* **92** 178701
- [46] Liu R R, Wang W X, Lai Y C and Wang B H 2012 Cascading dynamics on random networks: crossover in phase transition *Phys. Rev. E* **85** 026110
- [47] Miller J C, Slim A C and Volz E M 2012 Edge-based compartmental modelling for infectious disease spread *Soc. Interfaces* **9** 890–906
- [48] Miller J C and Volz E M 2013 Incorporating disease and population structure into models of SIR disease in contact networks *PLoS One* **8** e69162
- [49] Karrer B and Newman M E J 2010 Message passing approach for general epidemic models *Phys. Rev. E* **82** 016101
- [50] Strogatz S *et al* 1994 Nonlinear dynamics and chaos: with applications to physics, biology, chemistry, and engineering *Comput. Phys.* **8** 532